JMEPEG (2002) 11:651-658

Effects of Austempering Temperature on Fatigue Crack Rate Propagation in a Series of Modified (Cu, Ni, and/or Mo) Nodular Irons

M. Martínez-Madrid, M.A. Acosta, A. Torres-Acosta, R. Rodríguez-T, and V.M. Castaño

(Submitted 25 February 2002; in revised form 17 September 2002)

Studies on austempered nodular cast irons were carried out to establish the optimum isothermic heat treatment at a given chemical composition that rendered the highest fatigue crack propagation resistance. Seven nodular iron chemical compositions with different concentrations of copper, nickel, and or molybdenum were tested at three austempering temperatures achieving ausferritic microstructures. Three-point bend tests for crack growth rates were performed at room temperature in a close loop servo hydraulic machine. Crack opening displacement measurements were performed using a controlled displacement telescope. A simple linear statistical analysis indicated that the lower the austempering isothermal temperature, the higher the fatigue strength of the alloys. Cu and Mo additions along with a good spheroidicity of graphite nodules in the iron favored this effect.

Keywords ductile iron, fatigue cracking, lower ausferrite, nodular iron, nodularity percent, upper ausferrite

1. Introduction

Noticeable improvement of fatigue properties of nodular irons can be achieved through austempering heat treatment. This improvement can be such that these cast irons can advantageously compete with some forged steels in terms of fatigue properties—manufacturing cost mostly in automotive parts (i.e., crankshafts, gear shafts, etc.).[1-4] However, the combined effects of isothermal transformation temperature along with different alloying combinations on the fatigue cracking properties are still to be studied. Alloying combinations added to nodular iron such as Cu-Ni, Cu-Mo, Ni-Mo, and Ni-Mo-Cu are of particular interest for the manufacturing of commercial automotive components, because of benefits to the resulting mechanical properties. The effect of individual alloying elements, such as Mo, Ni, and Cu in nodular irons, has been reported elsewhere[5-12] and some combinations between these alloying elements have also been reported in other investigations.[1,12-15] However, no work was found relating these alloying combinations at different austempering temperatures and the resultant fatigue properties. As an example, notched impact testing, tensile strength, and fatigue testing of two nodular irons alloyed with Cu-Mo and Ni-Mo, reported by González et al.,[1] showed that both alloying combinations can render a better tensile strength and fatigue strength when austempered at 315 °C, thus developing a lower ausferrite microstructure than that at 370 °C showing upper ausferrite. Furthermore, Cu-Mo nodular irons rendered higher fatigue strength than Ni-Mo nodular irons.

It is necessary to mention that despite the similarity of austempering heat treatments between steel and cast iron, and due to the difference in microstructural constituents, the resulting phase for steel is named bainite, whereas that for iron is termed ausferrite.[1,15-17]

Ausferrite is an "acicular-like" ferrite supersaturated with carbon, with some retained austenite also saturated with carbon, surrounded by carbide precipitation.

2. Experiment

2.1 Nodular Iron Castings

Induction furnace melting nodularization followed by inoculation, and sand-mould casting was the regular foundry practice to produce the nodular irons tested.

The spheroidal form of carbon graphite of the cast ductile irons was produced by additions of magnesium (Mg) in the range of 0.05-0.06 wt.%. Since Mg is a highly reactive element at molten iron temperatures, sulfur and oxygen contents were kept as low as possible (<0.03%) in the molten iron. Fe-Si-Mg noduling agent particles (7% Mg) were made into compacts with metallic turnings and placed in a designed pocket to reduce the violent reaction with molten metal. The use of a cover with a tundish, through which the iron was poured, reduced fumes and the splashing of the metal, and improved the yield of Mg.

Final inoculation followed, using granular commercially available ferrosilicon containing 75% silicon (Si) inoculant. The amount of inoculant added was 0.5% in the ladle plunging it in a refractory bell.

Molten nodular iron alloys were then immediately cast onto Si sand (hardened with CO_2 and resins) Y-block type moulds followed by cutting and machining to get the necessary samples to be able to perform all chemical and mechanical tests as shown in Fig. 1. The resultant chemical composition of the

M. Martínez-Madrid, R. Rodríguez-T, and **V.M. Castaño,** Universidad Nacional Autónoma de México, Instituto de Física, Campus Juriquilla, Qro. 76230, México; and **M.A. Costa** and **A. Torres-Acosta,** Instituto Mexicano del Transporte, San Fandila, Pedro Escobedo, Qro. 76700, México. Contact e-mail: mmmadrid@servidor.unam.mx.

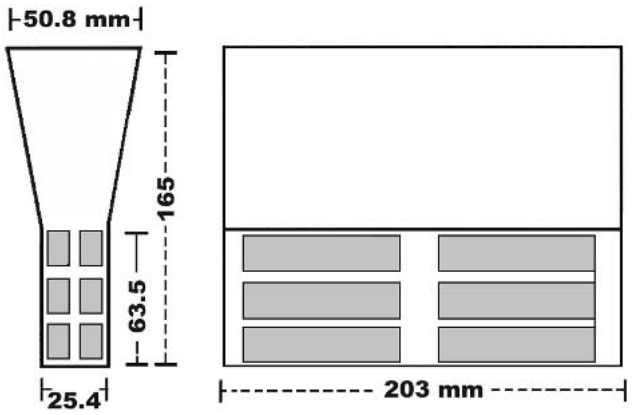

Fig. 1 Dimensions of Y block casting and location of mechanical testing samples

Table 1 Chemical Composition of Nodular Irons Tested, wt.%

Element/ Cast	C3	C4	C5	C6	C7	C8	C9 Unalloyed
C	3.660	3.880	4.110	3.880	3.690	3.740	3.720
Si	2.230	2.380	2.370	2.540	2.500	2.460	2.340
Mn	0.260	0.320	0.280	0.026	0.260	0.240	0.220
S	0.015	0.014	0.107	0.015	0.009	0.0066	0.007
P	0.024	0.024	0.022	0.022	0.021	0.210	0.020
Mg	0.047	0.045	0.030	0.062	0.037	0.049	0.041
Cu	0.660	0.100	0.140	0.640	1.000	0.410	0.090
Mo	0.253	0.237	0.167	0.044	0.261	0.315	0.045
Ni	1.010	1.020	0.634	0.884	0.048	0.039	0.037
Cr	0.052	0.041	0.055	0.044	0.043	0.032	0.032
Sn	0.008	0.007	0.010	0.007	0.007	0.007	0.007
Ti	0.003	0.003	0.008	0.008	0.006	0.006	0.006
Al	0.012	0.013	0.011	0.012	0.012	0.012	0.013

cast alloys is shown in Table 1. Please note that cast No. 9 is unalloyed and is used in this work as a blank sample.

2.2 Heat Treatment

All machined samples, protected with Zirconia paint and packed with gray iron turnings to prevent decarburization, were heated at 870 °C using an electric furnace for 2 h to achieve a fully austenite structure. Austempering was done at 370, 350, and 315 °C in molten salts of sodium nitrate. The samples were then held for 2 h to achieve upper ausferrite and lower ausferrite precipitation as shown in Fig. 2. Air-cooling followed.

2.3 Metallography Analysis

All samples were prepared for metallography analysis and etched with Nital 2%, observed under an Olympus PMG-3 (Olympus Optical Company, Ltd., Tokyo, Japan) microscope, and analyzed using a Buehler Omnimet IV (Buehler LTD., Lake Bluff, IL) image analyzer. Nodule assessment was performed without etching samples.

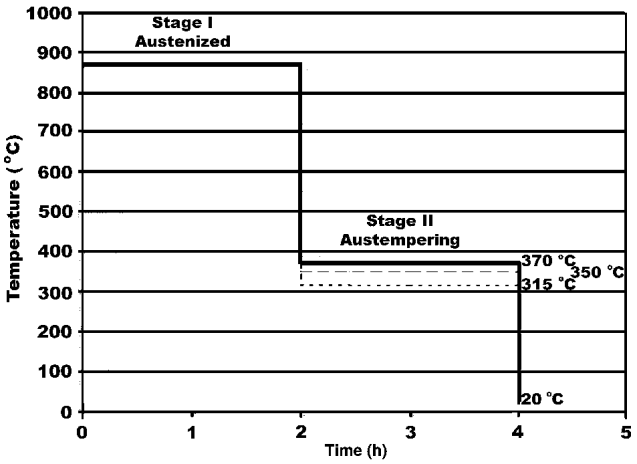

Fig. 2 Austempering heat-treatment conditions

2.4 Mechanical Testing

Uniaxial tensile strength was measured on each cylindrical type sample pairs (21 different combinations) following ASTM-399-90[18] using a MTS Servo-Hydraulic Machine model 810 (Instron Corp., Canton, MA).

Brinell Hardness tests were also performed on each sample using a 10 mm sphere indenter with an applied load of 2900 kg for 10 s. Hardness tests were performed on the samples used for metallography observation.

Fatigue crack growth rates were measured by testing sets of precracked 3-point bend samples (80 × 18 × 9 mm) per condition according to ASTM E647-88,[19] using the above-mentioned MTS machine. The fatigue samples were ground down and alumina polished to 0.005 mm to be able to visualize and measure the crack growth process during the fatigue testing. Forty-two samples were tested.

The precracking of all samples was performed starting with a K amplitude (ΔK) of 200 MPa$\sqrt{m}$, with a maximum load according to sample dimensions and initial crack size, of 6 KN and the minimum of 0.6 KN, based on the criterion that if after 100 K cycles no cracking developed, ΔK would have to be increased by 10%. The load to cycle profile applied to each test was sinusoidal. To measure the fatigue crack length as a function of the elapsed cycles, a stroboscope was used along with a 20-50× lens mounted on an aluminum rail frame, allowing X and Y displacement controlled by a micrometer. This setup was able to read crack lengths up to 0.036 mm (0.002 sample width).

The stress intensity factor, K, was calculated using the following expression:[20]

$$K = (PS/BW^{3/2}) \cdot f(a/W)$$

where the geometric factor was calculated using:

$$f(a/W) = \frac{3(a/W)^{1/2}\{1.99 - (a/W)\,[1 - (a/W)]\,\langle 2.15 - 3.93(a/W) + 2.7(a/W)^2\rangle\}}{2[1 + 2(a/W)][1 - (a/W)^{3/2}}$$

where P is load (kN), B is sample thickness (cm), S is support axes distance (cm), W is sample width (cm), and A is crack length (cm).

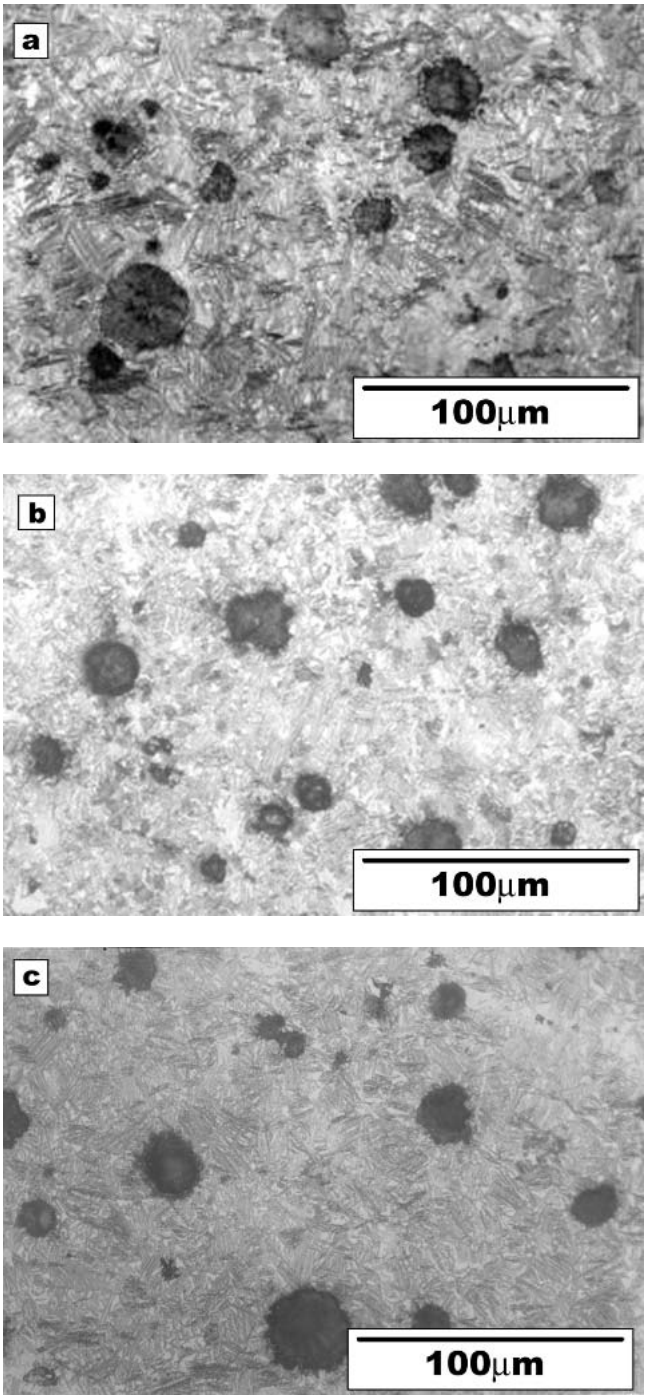

Fig. 3 Microstructures of C3 sample austempered at: **(a)** 315 °C, lower ausferrite matrix; **(b)** 370 °C, upper ausferrite matrix; **(c)** 350 °C, showing a mixture of ausferrites matrix

2.5 Fractographic Analysis

The cracking mechanisms were studied analyzing the fatigue-fractured samples. To assess the cracking front paths, the roughness changes, as well as the associated plastic front, an Olympus VHZ Stereomicroscope (Olympus) was used at 10-40×. To identify the type of fracture at the front of the crack

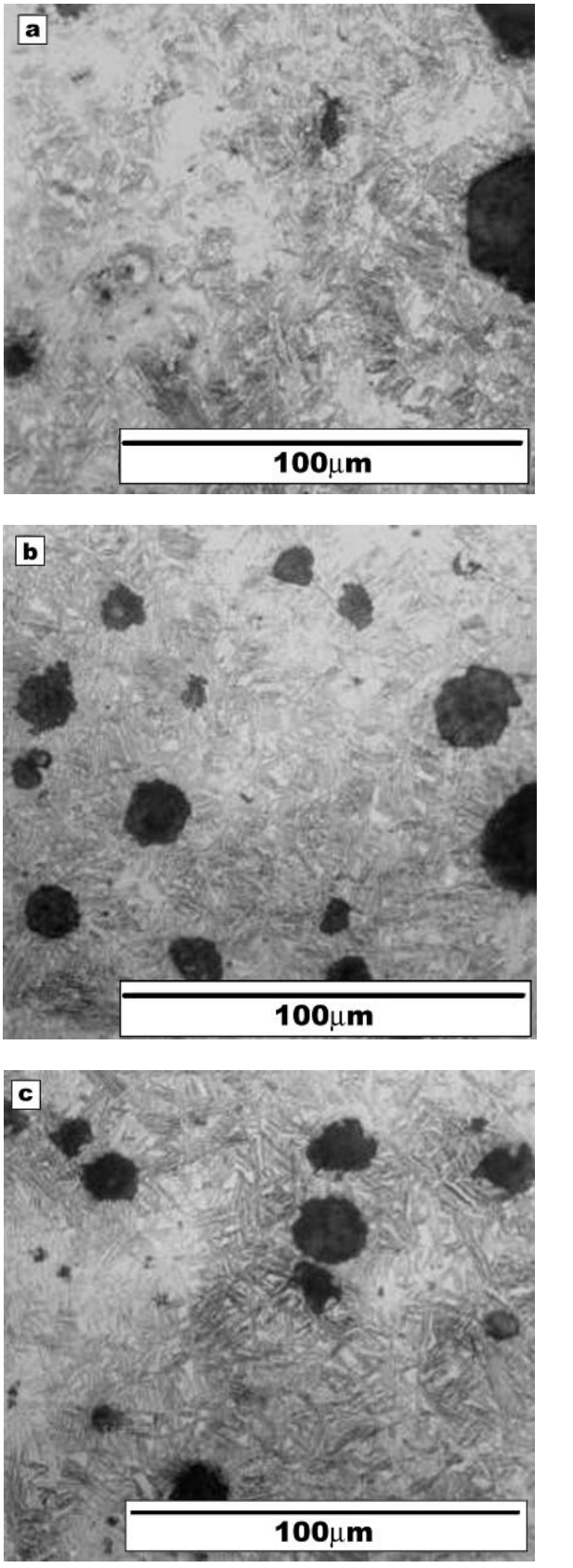

Fig. 4 370 °C austempered nodular iron microstructures with sample compositions: **(a)** C5, **(b)** C7, **(c)** C8

Table 2 Graphite Morphology

Alloy Composition	ASTM Size	Nodularity, %	Nodules/mm^2	Spheroidicity, %
1Ni0.25Mo.66Cu C3	6-7	95	155	68.1
1Ni0.24Mo0.1Cu-C4	5-7	80	211	65.9
0.17Mo0.63Ni0.14Cu C5	6-7	90	150	68.3
0.64Cu0.88Ni C6	5-7	90	280	82.8
1Cu0.26Mo C7	6-7	95	214	86.9
0.41Cu0.31Mo C8	5-6	85	180	75.6
Unalloyed-C9	6-7	95	280	82.1

displacement, a JEOL Scanning Electron Microscope (JEOL USA, Inc., Palo Alto, CA) at 20 kV accelerating voltage and secondary electrons was used. The overload failure area along with "high" and "low" ΔK areas were scanned.

3. Results and Discussion

Typical microstructures obtained from three different austempering temperatures for some sample compositions are shown in Fig. 3 and 4. As expected, fine lower ausferrite containing parallel lath shape units of ferrite was observed when austempering at 315 °C, whereas at 370 °C feather-like upper ausferrite developed. A mixture of both microstructures was obtained at 350 °C. The different chemical compositions of the casts did not render significant microstructural differences, although a higher amount of retained austenite was qualitatively observed in casts with 1% Ni than in those containing less concentration of Ni.

Table 2 shows the stereographic measurements of the precipitated graphite before heat treatment. No significant nodularity differences among the different casts were found. This is not the case with the spheroidicity and count rate results (nodules/mm^2), where differences of about 30% in spheroidicity among some casts were detected.

A summary of the average properties of the different casts tested is shown in Table 3. Generally, the lower the austempering temperature, the higher both the hardness and the ultimate tensile strength (UTS). Casts C7, C8, and C9 showed the higher strength of all casts. Each composition showed a good correlation coefficient on each specific mechanical property at the three different austempering temperatures. Note that unalloyed samples along with those samples having additions of Cu and Mo favored the highest R^2 value when testing uniaxially mechanical properties.

To assess the level of fatigue cracking resistance through the Paris equation, crack growth rates were plotted per sample and austempering temperature condition. Typical graphs obtained are shown in Fig. 5 and 6. Through a linear correlation and regression analysis, a slope and a R^2 value were calculated per sample under each testing condition. Even though the average values of the calculated slope are shown in Tables 4 and 5, the R^2 listed in these tables was calculated using all experimental data obtained after testing all samples per condition.

These calculated slope values can be related to the nodular iron susceptibility for fatigue cracking—the higher the slope value, the higher rate the crack travels in the nodular iron; thus the lower the resistance to fatigue cracking. To compare the results of all samples at different austempering temperatures and to obtain the metallurgical conditions that rendered the best fatigue resistance, the average slopes "*m*" or fatigue cracking susceptibility of the different cast compositions obtained per austempering condition were compared (Table 4).

Table 3 Average Mechanical Properties of Different Alloy Compositions at Three Austempering Temperatures

(a) Brinell Hardness, BHN

Alloy Composition	315 °C	350 °C	370 °C	R^2 (a)
1Ni0.25Mo0.66Cu-C3	372	310	274	0.97
1Ni0.24Mo0.1Cu-C4	375	318	275	0.96
0.17Mo0.63Ni0.14Cu C5	382	328	285	0.98
0.64Cu0.88Ni C6	390	326	303	0.96
1Cu0.26Mo C7	385	336	294	0.96
0.41Cu0.31Mo C8	393	336	289	0.95
Unalloyed-C9	385	344	303	0.95

(b) Yield Strength MPa

Alloy Composition	315 °C	350 °C	370 °C	R^2 (a)
1Ni0.25Mo0.66Cu-C3	1005	—	866	—
1Ni0.24Mo0.1Cu-C4	787	775	591	0.68
0.17Mo0.63Ni0.14Cu C5	1114	877	608	0.95
0.64Cu0.88Ni C6	864	725	557	0.93
1Cu0.26Mo C7	1091	813	654	0.96
0.41Cu0.31Mo C8	1007	880	724	0.92
Unalloyed-C9	1090	943	782	0.91

(c) Ultimate Tensile Strength, MPa

Alloy Composition	315 °C	350 °C	370 °C	R^2 (a)
1Ni0.25Mo0.66Cu-C3	1327	—	1136	—
1Ni0.24Mo0.1Cu-C4	1271	1053	834	0.95
0.17Mo0.63Ni0.14Cu C5	1350	1027	811	0.97
0.64Cu0.88Ni C6	1319	1020	820	0.97
1Cu0.26Mo C7	1359	1107	895	0.96
0.41Cu0.31Mo C8	1288	1069	937	0.96
Unalloyed-C9	1354	1157	951	0.97

(a) The squared correlation coefficient, R^2, was calculated using all samples tested data and not the actual average values shown in these tables.

It can be seen that alloys austempered at 315 °C showed the highest fatigue cracking resistance, whereas those samples treated at 370 °C presented the lowest fatigue resistance. Furthermore, sample C3 (1Ni-0.25Mo-0.66Cu) rendered the lowest fatigue cracking resistance at 350 and 370 °C, whereas samples C5 (0.17Mo-0.63Ni-0.14Cu), C7 (1Cu-0.26Mo), and C8 (0.41Cu-0.31Mo) proved to offer the highest fatigue properties (lowest "*m* slope") compared to the rest of the different chemical compositions austempered at 315 °C. The fact that

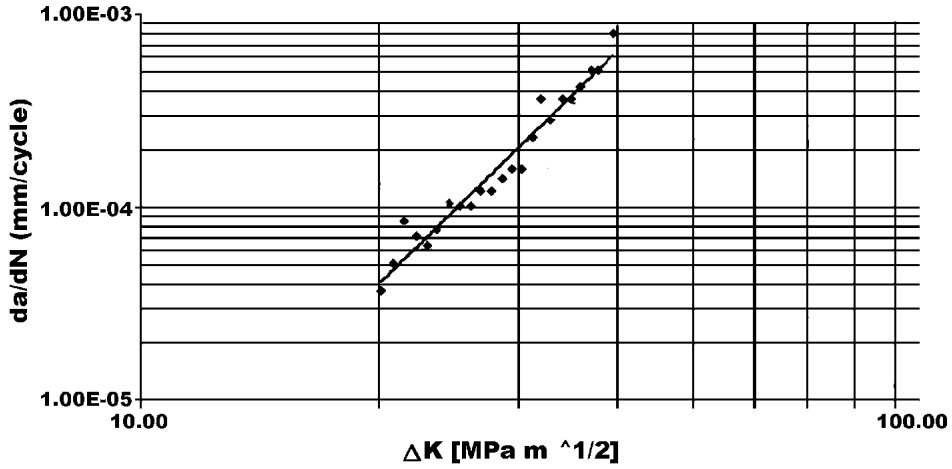

Fig. 5 Typical fatigue crack growth rate as a function of ΔK. Sample C7 austempered at 370 °C. Sample number 2 (y = 3E-10X $^{3.9961}$; R^2 = 0.9561)

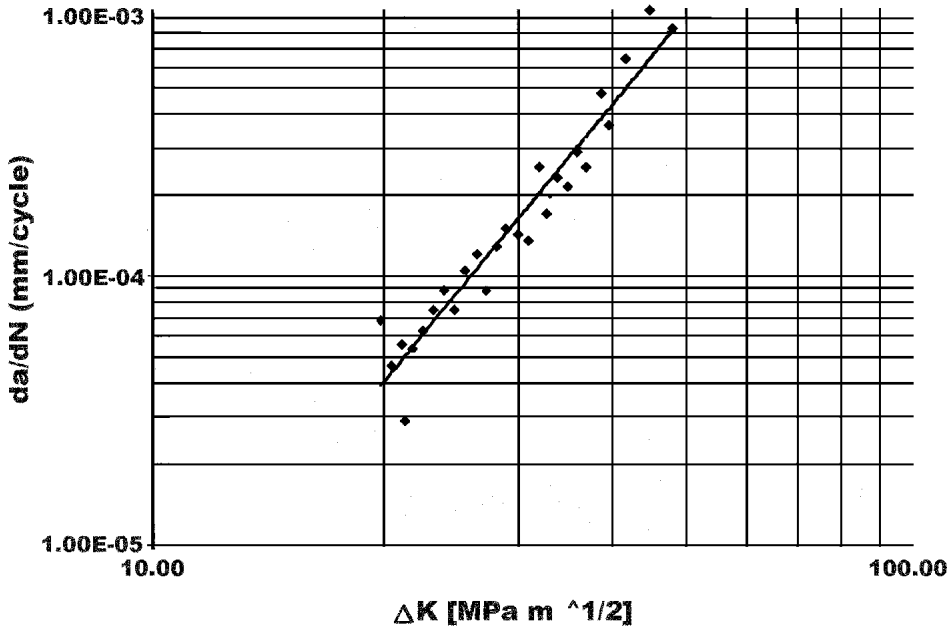

Fig. 6 Typical fatigue crack growth rate as a function of ΔK. Sample C3 austempered at 315 °C. Sample number 1 (y = 1E-09X $^{3.422}$; R^2 = 0.0318)

Table 4 Average Iron Susceptibility for Fatigue Cracking "m Slope" (According to Paris Equation) at Different Austempering Temperatures

Alloy Composition	315°C	350°C	370°C	R^2 (a)
1Ni0.25Mo0.66Cu-C3	3.45	3.85	4.62	0.86
1Ni0.24Mo0.1Cu-C4	3.57	3.76	4.50	0.78
0.17Mo0.63Ni0.14Cu C5	3.17	3.52	4.07	0.86
0.64Cu0.88Ni C6	3.54	3.24	4.08	0.83
1Cu0.26Mo C7	2.98	3.25	3.85	0.83
0.41Cu0.31Mo C8	3.27	3.51	3.92	0.89
Unalloyed-C9	3.60	3.57	4.06	0.55

(a) The squared correlation coefficient, R^2, was calculated using all samples tested data and not the actual average values shown in these tables.

these later chemical compositions also showed high R^2 values at the different austempering temperatures suggests that Cu and Mo additions are beneficial in both providing a better fatigue resistance and also rendering better ductile irons with predictable properties. This could be due to the increase of ausferriteability (equivalent to hardenability in steels)[1-5] in contrast with Ni that slows down the carbide precipitation.[9-11,13]

Fractographic analysis on each sample showed a typical fatigue fracture surface and the fatigue cracking propagation was achieved under the lineal elastic regimen. At low ΔK values, a pseudoclivage fracture type was developed and at high ΔK values, a larger plastic deformation of the matrix was observed, and even microvoid coalescence in the final cracking zone of sample C9 (blank) was developed as shown in Fig. 7.

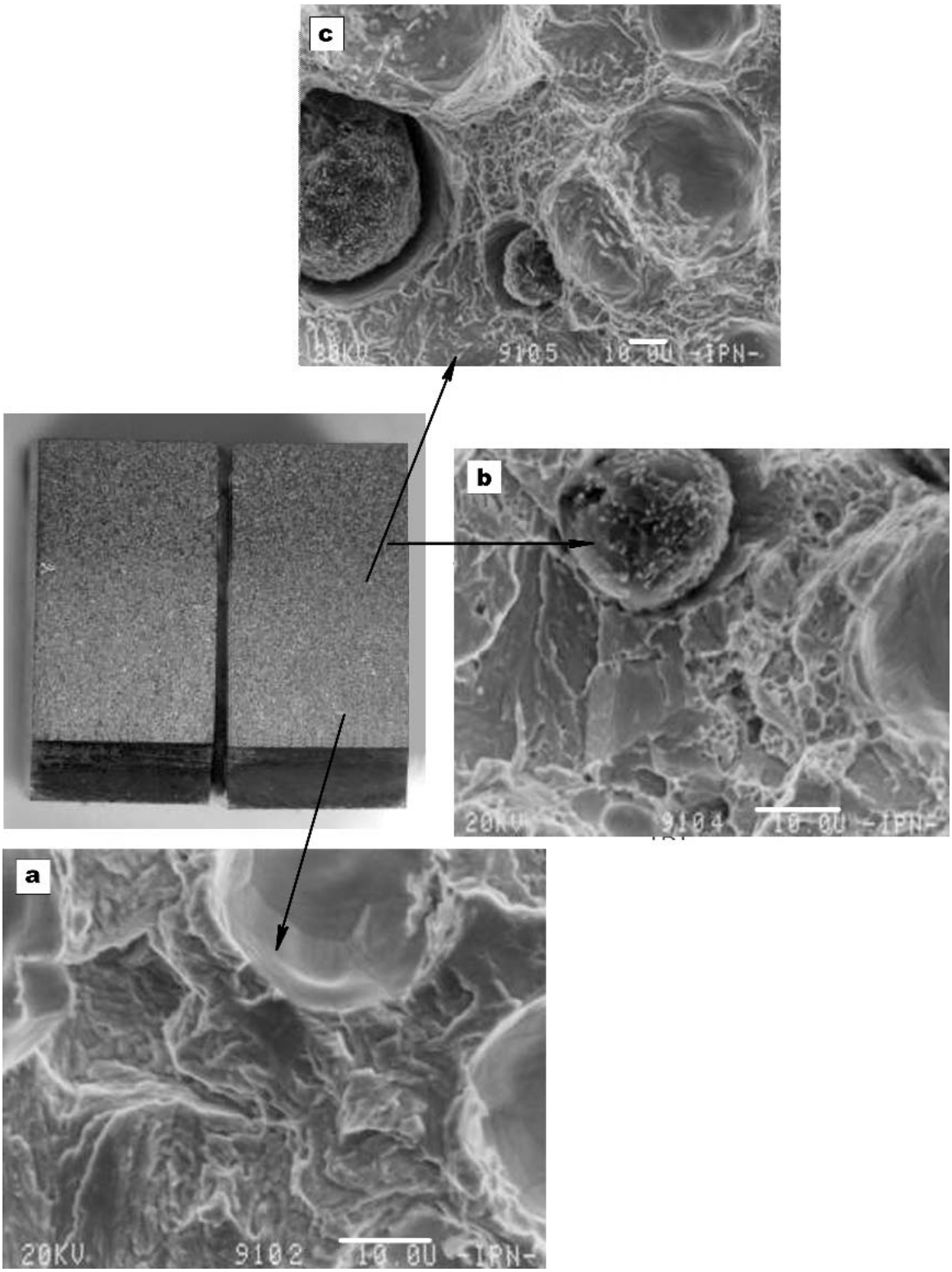

Fig. 7 Fatigue fracture surfaces of composition C-9 austempered nodular iron at 315 °C. The white arrow shows the crack displacement on the sample: **(a)** low ΔK pseudoclivage; **(b)** high ΔK rough surface and a mixture of fracture mechanisms; **(c)** final fracture zone, dimples.

No major fractographic differences on fracture features were appreciated throughout the different chemical compositions tested.

Even though the aim of this work was to study alloys organized as groups (Cu-Mo, Ni-Mo, Cu-Ni, and Cu-Ni-Mo) instead of varying alloy components systematically, a fatigue

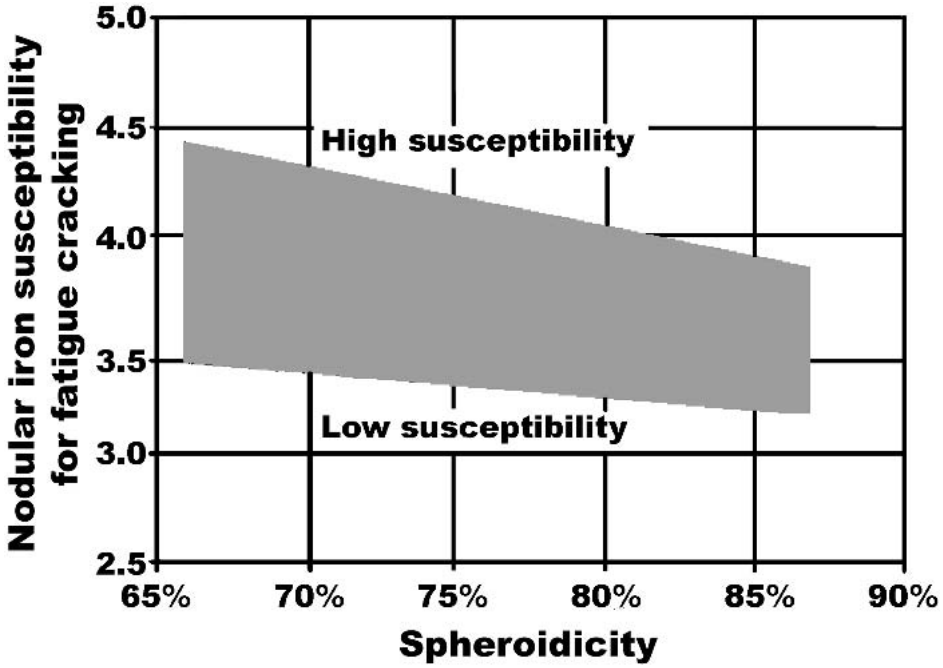

		Austempering Temperature,°C		
		315	350	370
Alloy Composition	Spheroidicity, %	Cracking Susceptibility Average "*m* Slope"		
C3	68.1	3.45	3.85	4.62
C4	65.9	3.57	3.76	4.50
C5	68.3	3.17	3.52	4.07
C6	82.8	3.54	3.24	4.08
C7	86.9	2.98	3.25	3.85
C8	75.6	3.27	3.51	3.92
C9	82.1	3.60	3.57	4.06

Fig. 8 Nodular graphite spheroidicity as a function of cracking susceptibility for fatigue cracking at different austempering temperatures. Data taken from Tables 2 and 4.

resistance improvement due to different austempering temperatures was achieved in some alloy groups.

Taking into account the cracking susceptibility (*m* slope values) obtained during the fatigue cracking analysis, the austempering temperatures proved to be significant on the different chemical compositions. Those compositions tested at 315 °C with a high R^2 consistently showed the lowest *m* values (highest fatigue resistance); whereas, those tested at 370 °C consistently proved to be the least fatigue resistant. The fatigue resistance of alloyed samples was increased in those irons with higher tensile strength. Alloyed ductile irons showing higher tensile strength also showed the best fatigue resistance performance. These results are in accordance with other trends reported elsewhere.[21-22,24,25] Apparently, Ni, Cu, and Mo additions to nodular iron austempered at 370 °C did not noticeably improve its fatigue cracking resistance compared with sample C-9 (unalloyed) despite an increase of tensile strength, as expected based on Forrest's[23] conclusions. However, under fatigue conditions, sample C-9 showed a poor R^2 throughout the three different testing temperatures, suggesting non-definitive conclusions. The Cu and Mo additions (1Cu-0.25Mo and 0.3Cu-0.3Mo) group of alloys showed the best fatigue properties. This is in agreement with previous work[1] and could be due to an improvement of ausferriteability by Cu and prompted by carbide formation precipitation of Mo.

No effect of nodularity percentage on the fatigue cracking susceptibility could be clearly established; however, an analysis of the spheroidicity values could suggest a possible trend with this susceptibility. Samples C6, C7, and C8 showing the highest spheroidicity percentages (>75%) also showed high R^2 coefficients (>0.83) and the lowest cracking susceptibilities. All three austempering treatments of these three compositions

showed the lowest susceptibility with the highest spheroidicity values. This behavior can be explained by a loss in the stress concentrations in a sphere-like nodule compared with a stress increase in nonspherical carbon nodules. Therefore, spherical nodules can act as crack arrest media, whereas no spherical nodules media can promote assisted cracking.

As previously mentioned, the highest susceptibility for cracking corresponds to both the minimum hardness and the yield point rendering the lowest fatigue resistance properties. From these data and as reported above, samples C-6, C-7, and C-8 showed the highest fatigue resistance and C-3 and C-4 the lowest of all. Comparing the results obtained with unalloyed nodular iron sample (C-9) and those alloyed, only three compositions provided better fatigue resistance: C-6, C-7, and C-8. This improvement in fatigue resistance was not as expected. So it can be concluded that a good fatigue resistance ductile iron can be achieved by alloying it with Cu and Mo, austempering at 315 °C, and assuring a good spheroidicity of carbon nodules. A technical issue to be considered when designing a ductile iron could be to guarantee that the ductile iron would have the right carbon content to ensure its austempering temperature to grant a lower ausferrite matrix, with spherical type carbon nodules.

4. Conclusions

- Austempering nodular irons at 315 °C proved to be more fatigue cracking resistant than at 350 or 370 °C.
- Because carbon nodules spheroidicity does not change with austempering temperatures, it is clear that the higher the spheroidicity, the less likelihood of fatigue cracking susceptibility. So taking into account the results shown in Tables 2 and 4, and considering that the microstructure does change with austempering temperatures, a proposed behavior of cracking susceptibility can be plotted as shown in Fig. 8. Thus, a lower ausferrite microstructure combined with high nodularity percentage should render a nodular iron of low fatigue cracking susceptibility or high fatigue resistance. Still, in this study, austempering nodular iron at 315 °C with high spheroidicity percentage is consistently less susceptible to fatigue cracking than austempering at higher temperatures and with lower spheroidicity percentage. Consistently, the better the nodularity, the better fatigue resistance at the three different austempering temperatures.
- In this research, a simple correlation analysis showed that the Cu-Mo group of alloys rendered the best fatigue cracking properties compared with other alloying combinations tested. The highest fatigue resistance was reached in those compositions showing the highest graphite nodularity percentage with high R^2 values.
- Assuring a spheroidicity value of carbon nodules as close to 0.85 as possible and austempering at 315 °C could favor a good fatigue cracking resistance of nodular irons.

References

1. J.L. González, J.M. Hallen, and M.M. Cisneros: "Resistencia Mecánica y a la Fatiga de Hierros Nodulares al Cu-Mo y Ni-Mo Austemperizados," *II Congreso Internacional de Materiales,* Instituto Tecnológico de Saltillo, Saltillo Coahuila. México, 1995, pp. 58-69 (in Spanish).
2. J.L. González and J.M. Hallen: "Resistencia a la Fatiga de Hierro Nodular Austemperizado," *Moldeo y Fundición Soc. Mexicana de Fundidores*, Año XVI, 1994, *96*, pp. 35-46 (in Spanish).
3. M.A. Acosta, M. Martínez Madrid, and J.A. López: "Efecto de la Temperatura de Austemperizado en la Velocidad de Crecimiento de Grietas en Hierros Nodulares Modificados con Cobre, Níquel y/o Molibdeno (Parte I: Desarrollo Experimental y Pruebas del Medio Continuo)," *Revista Latinoamericana de Metalurgia y Materiales,* 2000, *20*(1), pp. 3-12 (in Spanish).
4. M.A. Acosta, M. Martínez Madrid, and J.A. López: "Efecto de la Temperatura de Austemperizado en la Velocidad de Crecimiento de Grietas en Hierros Nodulares Modificados con Cobre, Níquel y/o Molibdeno (Parte II: Pruebas de Crecimiento de Grietas por Fatiga)," *Revista Latinoamericana de Metalurgia y Materiales*, 2000, *20*(1), pp. 12-22 (in Spanish).
5. A.J. Saldivar: *Efecto del Austemperizado Sobre la Microestructura y Propiedades Mecánicas del Hierro Dúctil Aleado con Níquel y Cobre,* Tesis de Maestría, Instituto Tecnológico de Saltillo, México, 1994, pp. 8-72 (in Spanish).
6. P.A. Blackmore and R.A. Harding: "The Effects of Metallurgical Process Variables on the Properties of Austempered Ductile Irons," *J. Heat Treating,* 1984, *3*(4), pp. 310-25.
7. R.C. Voigt and C.R. Loper: "Austempered Ductile Iron-Process Control and Quality Assurance," *J. Heat Treating,* 1984, *3*(4), pp. 291-309.
8. T.N. Rouns, K.B. Rundman, and D.M. Moore: "On the Structure and Properties of Austempered Ductile Cast Iron," *Am. Foundrymen's Soc. Trans.,* 1984, *92*, pp. 815-39.
9. K.L. Krishnaraj, H.N.L. Narasimhan, and S. Seshan: "Structure and Properties of ADI as Affected by Low Alloy Additions," *Am. Foundrymen's Soc. Trans.,* 1992, *100*, pp. 105-12.
10. B.V. Kovacs: "The Effects of Alloying Elements and Their Segregation in ADI," *Am. Foundrymen's Soc. World Conference on ADI*, 1991, pp. 241-70.
11. J.F. Janowak and R.B. Gundlach: "Development of a Ductile Iron for Commercial Austempering," *Am. Foundrymen's Soc. Trans.,* 1983, *91*, pp. 377-88.
12. R.E. Campos: *Estudio Cinético y Microestructural del Proceso de Austemperizado de Hierros Nodulares,* Tesis de Maestría, Instituto Tecnológico de Saltillo, México, 1993, pp. 21-42 (in Spanish).
13. J.F. Janowack and P.A. Morton: "A Guide to Mechanical Properties Possible by Austempering 1.5%Ni-0.3%Mo Ductile Iron," *Am. Foundrymen's Soc. Trans.*, 1984, *92*, pp. 489-98.
14. M.J. Pérez: *Elaboración y Tratamiento Térmico de Austemperizado de Hierros Nodulares Aleados con Cu-Mo,* Tesis de Maestría, Instituto Tecnológico de Saltillo, México, 1994, pp. 1-74 (in Spanish).
15. R.A. Prado: *Contribución al Estudio del Proceso de Austemperizado en Hierros Nodulares Aleados al Cu-Mo y Ni-Mo,* Tesis de Maestría, Instituto Tecnológico de Saltillo, México, 1995, pp. 1-14 (in Spanish).
16. C.H. Hsu and T.L.Chuang: *Metall. Mater. Trans. A, 2001*, *32A*(10), pp. 2509-13.
17. Anon.: "ASTM Designation A-644-96" in *Terminology Relating to Iron Castings,* Vol. 01.02. Infodisk, American Society for Testing and Materials, Philadelphia, PA, 1996.
18. Anon.: "ASTM Designation E 399-90" in *Standard Test Method for Plane-Strain Fracture Toughness of Metallic Materials,* American Society for Testing and Materials, Philadelphia, PA, 1990, pp. 509-39.
19. Anon.: "ASTM Designation E 647-88" in *Standard Test Method for Measurement of Fatigue Crack Growth Rates,* American Society for Testing and Materials, Philadelphia, PA, 1988, pp. 679-706.
20. M. García: *Propagación de Grietas por Fatiga en un Hierro Nodular Austemperizado,* Tesis de Ingeniero Metalúrgico, I. P. N., México, 1994, pp. 3-29 (in Spanish).
21. D. Broek: *Elementary Engineering Fracture Mechanics*, Martinus Nijhoff Publishers, 1987, pp. 99-309.
22. H.P. Van Leeuwen and L. Schra: *Heat Treatment Studies of Al Alloy 7079 Forgings*, Nat. Aerospace Inst. Amsterdam, TR 69058, 1969.
23. P.G. Forrest, ed.: *Fatiga de los Metales,* URMO, Spain, 1972, pp. 72-85 (in Spanish).
24. R.L. Donahue, H.M. Clark, P. Atanmo, R. Kumble, and A.J. McEvily: "The Effect of an Overload on the Rate of Fatigue-Crack Propagation Under Plane Stress Conditions." *Int. J. Fracture Mech., 8*, 1972, pp. 209.
25. A.J. McEvily: "On the Quantitative Analysis of Fatigue Crack Propagation, Fatigue Mechanisms: Advanced in Quantitative Measurement of Physical Damage," *ASTM STP 818,* J. Lankford, D.L. Davidson, W.L. Morris, and R.P. Wei, ed. American Society for Testing and Materials, Philadelphia, PA, 1983, pp. 283-312.